CSIRO PUBLISHING

International Journal of Wildland Fire **2016**, *25*, 547–557
http://dx.doi.org/10.1071/WF14078

Structure-level fuel load assessment in the wildland–urban interface: a fusion of airborne laser scanning and spectral remote-sensing methodologies

Nicholas S. Skowronski[A], *Scott Haag*[B], *Jim Trimble*[C], *Kenneth L. Clark*[D], *Michael R. Gallagher*[D] and *Richard G. Lathrop*[C,E]

[A]USDA Forest Service, Northern Research Station, 180 Canfield Street, Morgantown, WV 26505, USA.
[B]The Patrick Center for Environmental Research, Academy of Natural Sciences of Drexel University, 1900 Benjamin Franklin Parkway, Philadelphia, PA 19103, USA.
[C]Center for Remote Sensing and Spatial Analysis, Rutgers University, 14 College Farm Road, New Brunswick, NJ 08901, USA.
[D]USDA Forest Service, Northern Research Station, 501 Four Mile Road, New Lisbon, NJ 08064, USA.
[E]Corresponding author. Email: lathrop@crssa.rutgers.edu

Abstract. Large-scale fuel assessments are useful for developing policy aimed at mitigating wildfires in the wildland–urban interface (WUI), while finer-scale characterisation is necessary for maximising the effectiveness of fuel reduction treatments and directing suppression activities. We developed and tested an objective, consistent approach for characterising hazardous fuels in the WUI at the scale of individual structures by integrating aerial photography, airborne laser scanning and cadastral datasets into a hazard assessment framework. This methodology is appropriate for informing zoning policy questions, targeting presuppression planning and fuel reduction treatments, and assisting in prioritising structure defence during suppression operations. Our results show increased variability in fuel loads with decreasing analysis unit area, indicating that fine-scale differences exist that may be omitted owing to spatial averaging when using a coarser, grid-based approach. Analyses using a local parcel database indicate that approximately 75% of the structures in this study have ownership of less than 50% of the 30 m buffer around their building, illustrating the complexity of multiple ownerships when attempting to manage fuels in the WUI. Our results suggest that our remote-sensing approach could augment, and potentially improve, ground-based survey approaches in the WUI.

Additional keywords: Light detection and ranging (LiDAR), risk assessment, wildfire hazard.

Received 7 May 2014, accepted 16 July 2015, published online 10 September 2015

Introduction

The prevention and suppression of wildland fires within the wildland–urban interface (WUI) and intermix communities are of international interest. The amplified risk to life and property in these areas, increased complexity and costs of suppression (Liang *et al.* 2008) and mitigation activities (Berry and Hesseln 2004), the difficulty of evacuation, and the attitude and lack of social acceptance of residents (McCaffrey *et al.* 2012) are the primary drivers of this interest. Consequences of wildfires within the WUI have been dramatic, with notable examples occurring in Florida, USA (1998), California, USA (2003 and 2007), Greece (2007), Victoria, Australia (2009), and Texas, USA (2011). Five of the 10 most costly wildfire events in US history were within the WUI and each of these fires resulted in damages greater than $1 billion (USD, adjusted to 2010 dollars, NFPA 2010). In response, approximately USD 5.6 billion has been spent on hazardous fuel reduction to treat an average of $\sim$1 million ha year^{-1} over the last 10 years in the US alone (Gorte 2011; http://www.nifc.gov/fireInfo/fireInfo_documents/SuppCosts.pdf, accessed 22 July 2015).

Characterisation of fuel beds in the WUI is challenging because of the high spatial heterogeneity in fuel loads and fuel models (vegetative and structural fuels), human factors (perceptions, private ownership and social acceptance of mitigation activities), and increased property values at risk (Mell *et al.* 2010). As our effectiveness at mitigating fire risk in the WUI is explicitly tied to the prevention of structure ignition, analysis of fuels in this system should be focussed at the scale of the individual structure's home ignition zone (HIZ), defined as the area within 30 m of a structure (Cohen 2008). In the United States, the National Fire Protection Association (NFPA) has developed the Firewise Community Program to inform and guide public activities for mitigating wildfire risk of individual structures (http://www.firewise.org, accessed 22 July 2015).

Currently, the assessment of wildfire risk around individual structures in the United States is carried out through a ground-based visual assessment using guidance from NFPA standard 1144 (NFPA 2012). These surveys are time-consuming, potentially prone to subjective errors and limited in extent. An objective and consistent methodology for deriving critical parameters at larger scales yet incorporating the resolution of individual structures would greatly increase our capacity to perform meaningful analyses and make informed management decisions.

Numerous studies have characterised and then classified vegetation into fuel models (e.g. Scott and Burgan 2005) using spectral reflectance data (e.g. Arroyo *et al.* 2008; Alonso-Benito *et al.* 2013) at varying spatial resolutions. Koetz *et al.* (2008) used a fusion approach to link spectral reflectance data and airborne laser scanning (ALS) to classify a highly variable landscape that included WUI areas, and they reported an improvement in the classification of strata relative to the use of spectral reflectance data alone. More recently, and specific to the WUI, Platt (2014) presented an object-oriented analysis based on the HIZ of individual structures that estimates and then ranks relevant wildland fire exposure characteristics. Although these classification studies have illustrated a high degree of accuracy with regard to identifying the type of fuel, quantifying the amount of fuel remains challenging. Several studies have demonstrated the utility of light detection and ranging (LiDAR), specifically ALS, data for estimating canopy bulk density (CBD; Andersen *et al.* 2005) and vertical arrangement of fuels at landscape scales (Skowronski *et al.* 2007, 2011). A fusion of ALS and spectral reflectance data has also been shown to provide additional accuracy for vegetation classification and loadings estimation (e.g. Mutlu *et al.* 2008 ; Erdody and Moskal 2010; Jakubowksi *et al.* 2013).

Here, we present a systematic methodology for estimating fuel characteristics and loading within the HIZ of individual structures. The objective of this study was to develop a methodology for using emerging remote-sensing products and analysis techniques to characterise fuel loads and wildfire hazard in the WUI. This resulting methodology is objective, repeatable and appropriate for informing zoning policy, targeting presuppression planning and fuel reduction treatments, and assisting in prioritising structure defence during suppression operations. Specifically, we used a combination of high-resolution multispectral imagery and ALS data along with an object-oriented fuel classification routine to quantify three-dimensional fuel loads within 30 and 91 m and for each land parcel of 5500 individual structures over a 40-km^2 area. We integrated the results of this analysis into a conceptual hazard model that allowed a simplistic and operationally useful assessment of structures at risk. Finally, we assessed the proportion of structures that require the co-management of fuels on adjacent parcels by calculating the percentage of the ignitability zone around homeowners' properties.

Methods

Study area

The study focussed on several high-risk subdivisions located in and adjacent to the New Jersey Pinelands National Reserve (PNR), a predominantly forested area of ~445 000 ha in southern New Jersey, USA (Fig. 1). Development within the PNR has been limited by the Pinelands Protection Act of 1979 (Pinelands Commission 1980), but large areas of urban interface and intermix exist immediately adjacent to the PNR (La Puma *et al.* 2013). The study area includes several planned communities (Ocean Acres, Brighton at Barnegat, Pinewoods Estates) and several individual homes in Stafford and Little Egg Harbor townships in Ocean County, NJ, that occur within this adjacent area.

Forest communities in the study area are characterised by a mixture of pine-dominated (*Pinus rigida* Mill. and *P. echinata* Mill.) and oak-dominated (*Quercus alba* L., *Q. coccinia* Muench. and *Q. prinus* L.) overstories (McCormick and Jones 1973). The understorey is composed of shrubs, primarily *Vaccinium* spp., *Gaylussacia* spp. and *Kalmia* spp. Forests in the PNR are typically characterised using the SH8 fuel model from the Scott and Burgan models (Scott and Burgan 2005) or Fuel Model 'B' from the Anderson (Anderson 1982) fuel models. Soils are derived from the Cohansey and Kirkwood formations and are coarse, sandy, nutrient-poor and well drained (Tedrow 1986).

Forests in the PNR are fire-adapted and crowning fire behaviour can occur during wind-driven wildfire events. Wildfire occurrence peaks in the spring, before green-up. New Jersey has a 10-year mean fire frequency (2003–13) of 1260 ± 831 (mean $\pm$ standard deviation throughout) wildfires year^{-1} with an average area burned of 2014 ± 2974 ha year^{-1}, with a vast majority occurring within the PNR (http://www.nifc.gov/fireInfo/fireInfo_statistics.html, accessed 22 July 2015). Over the same period, 124 ± 37 prescribed fires year^{-1} were conducted on an average of 4896 ± 2216 ha year^{-1} (http://www.nifc.gov/fireInfo/fireInfo_stats_prescribed.html, accessed 22 July 2015). Over the last 100 years, fire size has decreased from an average of 45 ± 8.2 ha, before 1940, to 6.4 ± 1.3 ha, mostly owing to decreased response times and advances in suppression technology (Forman and Boerner 1981). However, recent events have illustrated the continued risk of fire in this system and include high burned area totals and structure losses, including the 2007 Warren Grove (6273 ha) and the 2002 Jake's Branch (517 ha) wildfires. The rapid spread of these fires reduced the effectiveness of structure protection operations and further demonstrated the need for effective presuppression fuels management in the communities in and around the PNR. Several of the communities used in our analysis experienced structure loss and damage during the Warren Grove wildfire (4 structures destroyed and 37 damaged).

Approach

Our general approach was to treat each structure as an analysis unit and examine the fuel conditions around each at distances of 30 and 91 m (corresponding with NFPA guidance and our validation data; Fig. 2), and at the level of the land parcel associated with each structure. Fuel types were classified using an automated image-segmentation technique, fuel loads were estimated using ALS data and previously developed canopy fuel models, fuel classification was assessed by the percentage of pine canopy within each buffer, and the homeowner's ability to directly impact fuels was evaluated by estimating the percentage of each

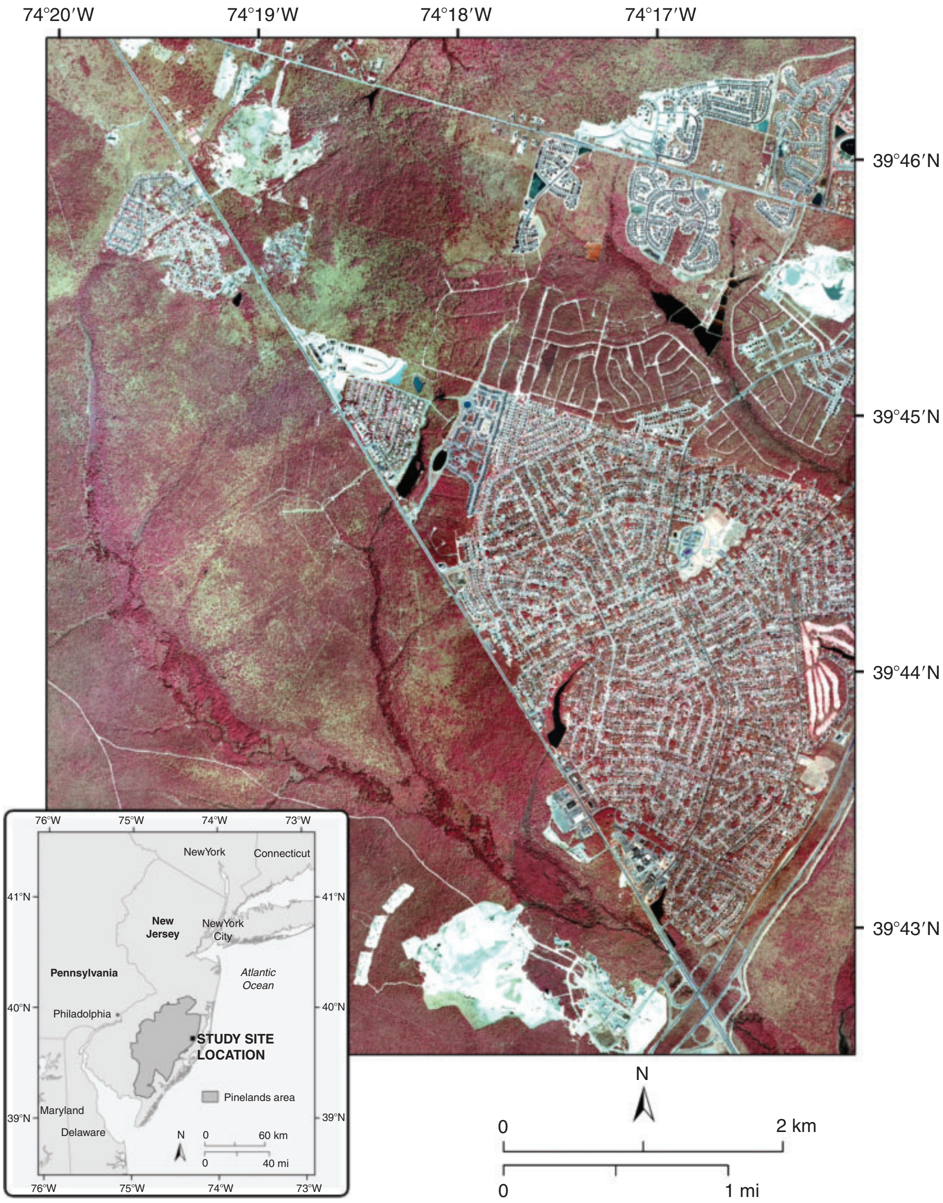

Fig. 1. Map of New Jersey Pinelands study site. The inset shows the location of the New Jersey Pinelands, and the larger map shows the details of the study site.

structure's buffer that was within the associated ownership parcel. We evaluated these remotely sensed estimates using field-collected hazard assessment data. Finally, we developed a simple model to evaluate fire hazard for each structure based on these metrics.

Datasets

High-spatial-resolution colour infrared digital orthophotography (CIR; 0.3×0.3-m ground resolution) was acquired in March 2007 (from the State of New Jersey Office of Information Technology, Office of Geographic Information Systems, Trenton, NJ) and used to classify and map fuels. To estimate three-dimensional fuel structure, ALS data were acquired in October 2008 during leaf-on conditions with a Leica ALS 60 (Leica Geosystems AG, Heerbrugg, Switzerland) flown on a fixed-wing aircraft at ~1100 m above ground level. The resulting pulse footprint size of the ALS data was ~0.25 m, with an average density of 3.6 ± 1.7 pulses m^{-2}, and a return density of 4.6 ± 2.2 returns m^{-2}. Up to four returns per pulse were digitised. A total of 5569 individual structures were hand-digitised from colour orthophotos that were acquired during the ALS acquisition. To be consistent with field-collected hazard assessments (described below), we created 30- and 91-m radial buffers (B_{30} and B_{91} respectively) around each structure in a geographic information system (GIS). The mean areas were 0.4 ± 0.1 and 2.6 ± 0.3 ha for B_{30} and B_{91} respectively. The radial buffers varied in area because they were constructed from the edges of the each structure. As a comparison with the

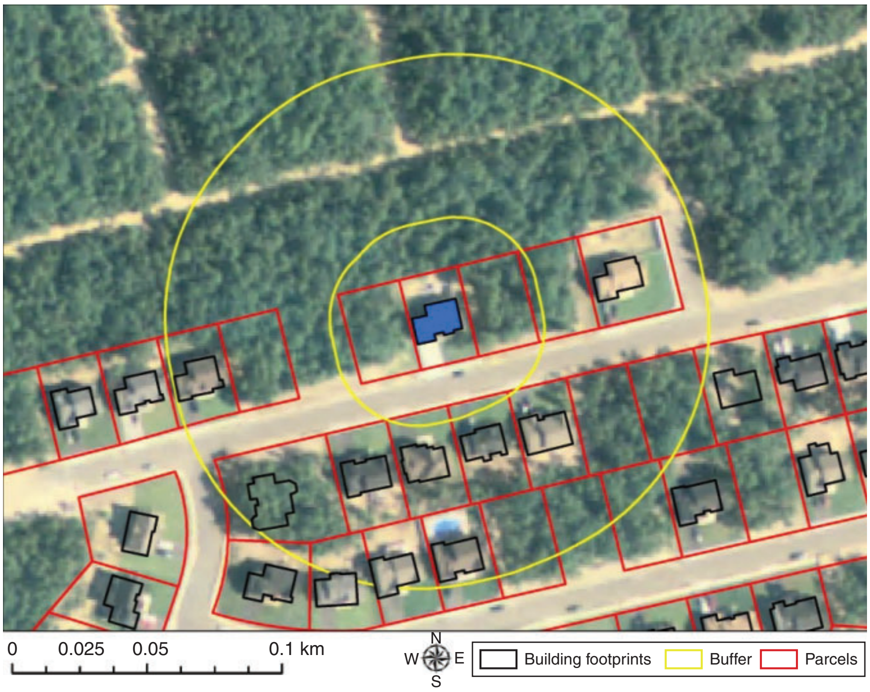

Fig. 2. An example of the analysis window used around each structure to characterise fuel classification and loading in the home ignition zone (HIZ). Parcels are shown for each building within the figure. Both 30-m (B_{30}; inner circle) and 91-m (B_{91}; outer circle) buffers are shown for an individual structure (in blue).

fixed-radius method, we linked a land ownership parcel geodatabase that was acquired from the Ocean County, New Jersey, Department of Planning (http://www.planning.co.ocean.nj.us/GIS.htm) to each structure. The parcels (P) had a mean area of 0.2 ± 0.8 ha. B_{30}, B_{91} and P were used to extract variables from the ALS dataset and the forest cover map. Structure footprints within B_{30}, B_{91} and P were excluded from all analyses.

Fuel classification

The colour infrared digital orthophotography was used for mapping fuel classes. We used a multiresolution image-segmentation approach in the *eCognition* image analysis software (Trimble Geospatial Imaging, Westminster, CO; standard version 5.0). The software uses a bottom–up region-merging technique to generate homogeneous objects through a local optimisation procedure. Four multispectral imagery bands and a 1×1-m-resolution canopy height model, derived from the ALS data (described below), were included in the segmentation process (described below). Objects were classified as tree (including shrub), lawn or impervious surface (roads, driveways, sidewalks or buildings) with a Random Forest classification and regression tree (CART) method, implemented using the 'TreeBagger' routine of the *Matlab* software package (Mathworks, Natick, MA; www.mathworks.com/help/stats/treebagger-class.html). Random Forest is an ensemble learning method that constructs a multitude of decision trees as part of the training process and provides outputs of modal class for nominal data, or mean prediction regression for numeric data of the individual trees (Breiman 2001). As conifer- or evergreen-dominated vegetation in close proximity to structures is of concern owing to its greater flammability relative to deciduous forest types, pixels classified as 'tree' were further stratified into deciduous or coniferous classes using the TreeBagger routine. A random sample of 300 points was classified into the appropriate land-cover category by visual interpretation of the CIR aerial photography, and then used to train the Random Forest Model. We employed 'leaf-off' imagery (acquired March 2007) to be able to easily discriminate between evergreen conifer and leaf-off deciduous canopy cover. We used this as a simple analogue of fuel flammability, with pine (evergreen) being more flammable than oak (deciduous).

Fuel loading

The ALS data were used to estimate fuel loadings within B_{30}, B_{91} and P. The ALS data were processed to classify 'ground' and 'canopy' returns using the filtering routine in the 'Toolbox for LiDAR Data Filtering and Forest Studies' (*TiFFS*; Chen 2007). We then built a continuous, 1×1-m horizontal-resolution digital elevation model (DEM) from the ALS dataset for the study area. Similarly, we estimated a corresponding 1×1-m canopy height model (CHM) using the *TiFFS* software package for use in the image segmentation and classification process described above. Using the DEM as a ground reference, the z-coordinate of each ALS return was recoded from height above mean sea level to height above ground. A height distribution of first returns was then calculated for each B_{30}, B_{91} and P in 1-m vertical

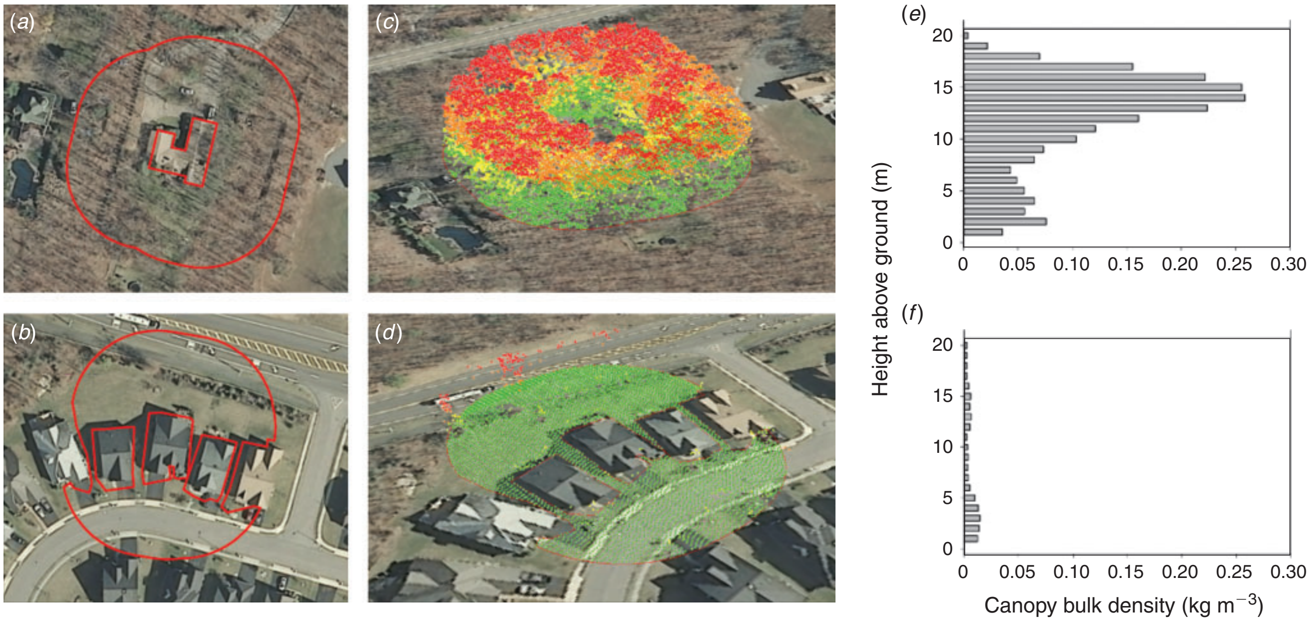

Fig. 3. Example of individual structure with high loading (*a*), and with low loading (*b*) with 30-m buffer from colour orthophoto. Corresponding example of airborne laser scanning (ALS) point-cloud for high loading (*c*), and low loading (*d*). Graph of canopy bulk density (CBD) for high-loading (*e*), and low-loading examples (*f*).

increments (e.g. Fig. 3). We selected this sampling scheme to eliminate the effects of placing a regular grid over an irregular pattern where individual structures would not be registered on the centroid of a cell. The distribution was calculated above 1 m to minimise the inclusion of returns misclassified as 'ground' because of shrubs, downed trees and other factors that would lead to these errors of commission by the ground-finding algorithm. Because canopy components may be obstructed by vegetation from above, they can be underestimated in the ALS dataset. To account for any potential occlusion, the height distributions were transformed using methods presented in MacArthur and Horn (1969) and applied to ALS data (Skowronski *et al.* 2007, 2011).

Canopy fuel distribution and loadings were estimated from the ALS estimated height distributions for each buffer using canopy fuel models developed in Skowronski *et al.* (2011) and Clark *et al.* (2013). They calculated estimates from both allometric models and destructive sampling of CBD profiles (CBD_{bin}) for field plots that were spatially and temporally coincident with an ALS acquisition, where discrete values are estimated for each 1-m vertical height bin. They then developed models to estimate CBD profiles using the ALS distribution variables as ancillary data. Here, we used these models to estimate CBD profiles for each B_{30}, B_{91} and P. To simplify the expression of these profiles, we estimated three variables (Table 1): CBD_{max} (maximum CBD; kg m^{-3}), CFL (canopy fuel load, sum of all CBD_{bin}; kg m^{-2}), and CBD_{Ladder} (sum of CBD_{bin} between 1 and 3-m height; kg m^{-3}).

We initially compared the ALS-estimated fuel loadings with estimates made of aerial photo-interpreted forest cover. First, a random sample of 90 structures was selected. Four of these structures showed a change in fuel loading between the acquisition of the March 2007 aerial photography and the October 2008 ALS acquisition due to the Warren Grove wildfire (three of the structures) and because of new construction (one structure); these were omitted from consideration. Owing to a software limitation that did not allow data extraction across all ALS tiles, B_{91} was not extracted for 19 of the selected buildings, resulting in a sample size of 67 (rather than the sample size of 86 for B_{30}). Using the 2007 leaf-off colour infrared photography, we interpreted and digitised forest cover for the selected structures. Percentage forest cover was calculated and compared with the ALS-estimated CFL for each structure subsample.

Table 1. Variables estimated for individual 30-m radius (B_{30}) and 91-m radius (B_{91}) buffers

Estimated variable
Percentage conifer forest ($\%_{conifer}$; %)
Maximum canopy bulk density (CBD_{max}; kg m^{-3})
Total canopy fuel load (CFL; kg m^{-2})
Ladder fuels (CBD_{Ladder}; kg m^{-3})
Percentage of buffer within ownership parcel ($\%_{ownership}$; %)
Distance to contiguous forest (ContigDist; m)

The second evaluation method employed visually estimated vegetation density from structure assessments performed by New Jersey Forest Fire Service (NJFFS) personnel as a part of the NJFFS Wildland Risk & Hazard Assessment survey. These data were collected for individual structures using a form adapted from NFPA 1144: Standard for Reducing Structure Ignition Hazards from Wildland Fire (NFPA 2012). The assessments recorded several risk factors including: means of access, available fire protection, vegetation, topography, fire history, building construction materials and utility placement. A field observer visually assessed each structure in the study area and ranked the fuel loads as: 0 – Light, 5 – Moderate, 15 – High and 25 – Extreme. Assessments were performed by NJFFS personnel during the summers of 2009 and 2010, and provided over 3800 individual-structure records. Results from this field survey were entered into a geodatabase so they could be spatially merged with remotely sensed data products and then directly compared with the results from the ALS-assisted fuel load estimation in B_{30}, B_{91} and P.

Spatial characteristics

We used the output generated from the fuels classification and fuel loading estimation to estimate several variables for B_{30}, B_{91} and P (Table 1). The proportion of coniferous cover and fuel loading variables (as estimated above) were computed for each structure. We also estimated an individual structure's distance from spatially adjacent or contiguous forests. First, we delineated large (>5 ha), spatially connected patches of forest within the study area. We then calculated each building's distance from the edge of these contiguous patches of forest and recorded it for each structure (ContigDist). Structures that were closer to the edge of the study area than to contiguous forest were excluded. To assess an owner's ability to manage fuels within the HIZ of their structure without assistance from adjacent property owners, we calculated the proportion of the B_{30} and B_{91} buffers that fell within the parcel of each structure.

Risk analysis

Several of the remotely sensed variables were combined to create a 'relative' risk model (i.e. relative to the information presented here rather than any 'universal' risk standards). We used expert judgment to develop a composite model that weighted and combined several of the estimated variables for the B_{30} and B_{91} buffers. Thus, the model integrated several of the key variables that define an individual structure's risk, and it provided a synthetic output that could be used to allocate both presuppression and suppression resources. Several of the variables estimated for each buffer were extracted and binned into three equal size classes, which were labelled as low, medium and high. The model used these ranked classifications to define a relative degree of risk for each structure as:

$$\text{Risk} = (0.5\text{CBD}_{\text{Ladder}}) + (0.5\text{CFL}) + (\%\ \text{coniferous}) + (2\text{ContigDist}) \quad (1)$$

The composite risk model was then binned into five categories from lowest to highest risk. The composite risk model was run at a grid-cell resolution of 15 × 15 m.

Results

Fuel classification

Buffer size did not have a large effect on the percentage of coniferous cover adjacent to individual structures, with both sizes exhibiting similar distributions (Table 2). The majority of structures had 0–10% coniferous cover in B_{30} (73.4%) and B_{91} (87.9%; Table 2). When data were analysed by parcel, the majority of structures (24.8%) had 10–20% coniferous cover (Table 2). Although 32% of the parcels had >30% coniferous cover, only 2.8 and 1.5% of B_{30} and B_{91} respectively were above this threshold (Table 2). When collapsed into three classes, the spatial patterning was generally homogeneous at the local scale between structures, but variable across the entire study area (Fig. 4*a*).

Table 2. Percentage of parcels, B_{30} and B_{91} by class of percentage coniferous forest ($\%_{\text{conifer}}$)

% conifer	Parcel	B_{30}	B_{91}
0–10	23.2	73.4	87.9
11–20	24.8	17.4	6.9
21–30	19.6	6.4	3.7
31–40	16.1	2.0	1.0
41–50	8.4	0.8	0.5
51–60	4.0	0.0	0.0
>61	3.9	0.0	0.0

The distance of structure centroids to contiguous forest areas was bimodal, with the largest peak of structures (19.7%) within 30–91 m of contiguous forests, and an additional peak (19.6%) occurring in the 305–610-m class (Table 3). Over one-third of the buildings were within 91 m of the contiguous forest matrix (Table 3; Fig. 4*b*). This distribution can be illustrated when the data are presented spatially, and it is apparent that the relative size of housing clusters is the driving factor (Fig. 4*b*). The relative maximum of the distribution at 305–610 m is a result of the homes in the large development in the south-eastern portion of the study area, whereas the absolute maximum at 30–91 m is a result of an integration of several smaller housing clusters throughout the study area and the presence of structures that are in that range within the large housing cluster (Fig. 4*b*).

Fuel loading

Results of the ALS-estimated fuel loading for P, B_{30} and B_{91} are shown in Table 4. For CFL, CBD_{max} and $\text{CBD}_{\text{Ladder}}$, the areal sampling methods are in agreement with the fuel range where the maximum proportion of structures occurred: 0.1–0.2, 0.01–0.02 and 0.02–0.03 kg m^{-3} respectively. The ranges of these distributions became more condensed as the area that the ALS returns were integrated over became larger (P being the smallest and B_{91} the largest areal units, on average (Table 4)). The spatial pattern of CBD and ladder fuel varies across the study area, with notable 'hotspots' of higher canopy fuel loading and ladder fuels occurring in isolated geographic areas (Fig. 4*c*, *d*).

Although CBD and percentage forest cover are not the same characteristic of forest structure, they are highly correlated. When ALS-derived CBD measurements were compared with the photo-interpreted forest cover within the B_{30} buffer for the random sample of structures, a strong linear relationship resulted ($R^2 = 0.66$; Fig. 5). However, grouping CFL for B_{30}, B_{91} and P by field-estimated fuel class illustrates no differences of mean CFLs between the 'moderate' and 'high' classes or areal unit (Fig. 6). In these classes, the standard deviations again vary based on the size of the aerial unit, with P having the largest amount of variability and B_{91} having the lowest (Fig. 6). For the 'extreme' class, the mean values are different between each of the areal units, with P having the lowest average CFL and B_{91} the highest (Fig. 6).

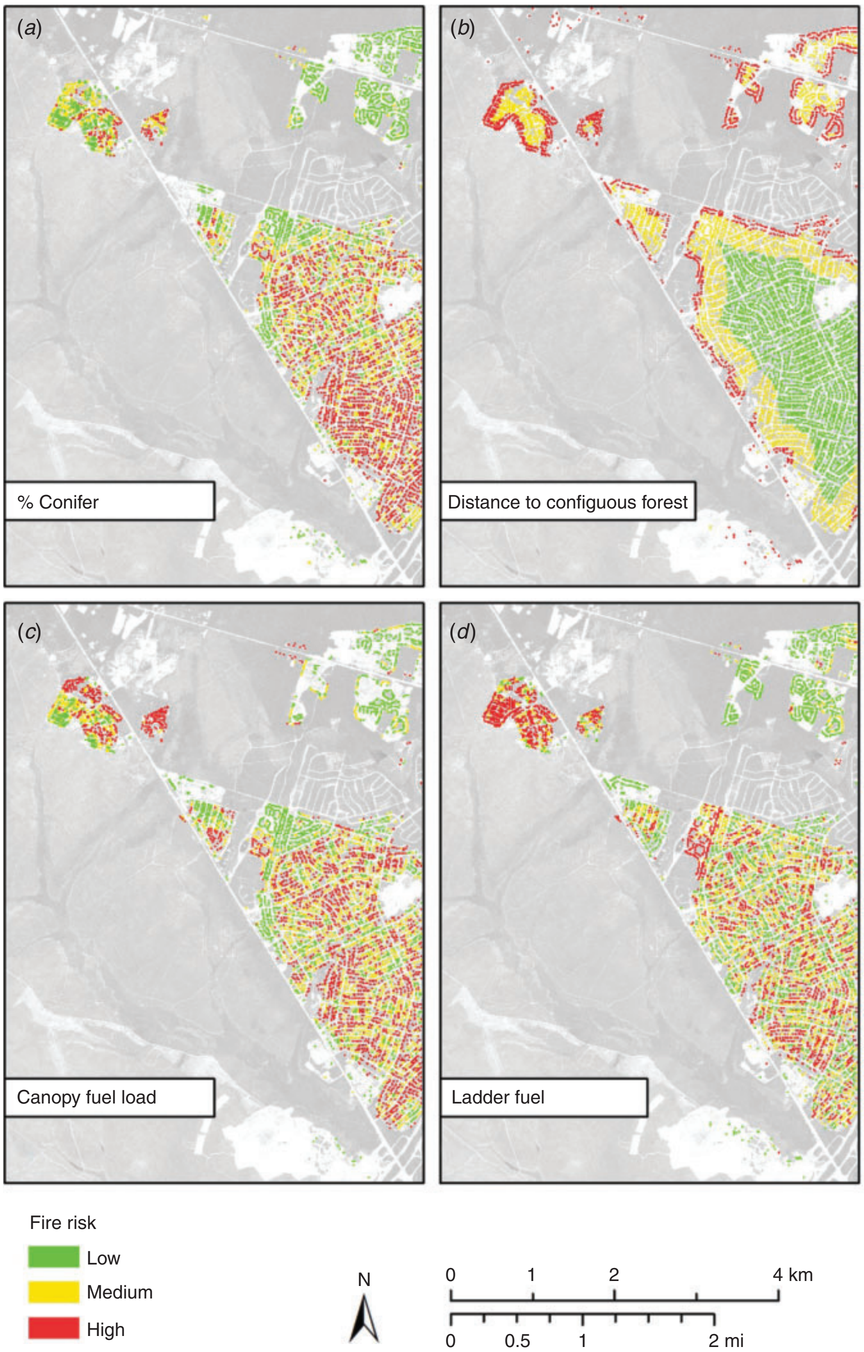

Fig. 4. Categorised maps of (*a*) percentage conifer cover; (*b*) distance to contiguous forest; (*c*) canopy fuel load (CFL); and (*d*) ladder fuel for B_{30}.

Home ignition zone and risk analysis

For the HIZ, we assessed the percentage of area within the B_{30} buffer that was included in the ownership parcel. Over 75% of the structure centroids can be considered to have limited flexibility for owner-initiated fuels management because less than 50% of the B_{30} buffer is within the associated ownership parcel (Fig. 7). We should note that some of the structure centroids do not always represent the primary residence but may represent outbuildings that may be at the edge of parcels; thus, these outbuildings may show up as having a lower percentage of B_{30} within the ownership parcel. This analysis is also somewhat confounded because of the presence of several large single-ownership parcels with rental spaces for individual residences (Fig. 8*b*), which had 100% of B_{30} within the large parcel, potentially misrepresenting the ability of individual homeowners to manipulate fuels in this area.

Table 3. Percentage of building centroids by distance to contiguous forests ($DIST_{contig}$)

ContigDist (m)	% of centroids
0–30	15.1
31–91	19.7
92–153	11.7
154–229	10.1
230–305	6.3
306–610	19.6
611–915	12.6
>916	4.9

Table 4. Percentage of parcels, B_{30} and B_{91} buffers by amounts of crown fuel weight (CFL), canopy bulk density (CBD_{max}) and ladder fuels (CBD_{Ladder})

Variable	Range	Parcel	B_{30}	B_{91}
CFL (kg m^{-2})				
	0.00–0.10	22.6	9.1	2.4
	0.11–0.20	37.2	53.6	48.4
	0.21–0.30	24.7	32.8	45.4
	0.31–0.40	10.0	4.2	3.8
	0.41–0.50	3.8	0.2	0.0
	0.51–0.60	1.0	0.1	0.0
	>0.61	0.7	0.0	0.0
CBD_{max} (kg m^{-3})				
	0.000–0.010	5.7	9.2	7.0
	0.011–0.020	44.6	67.1	79.3
	0.021–0.030	28.7	19.9	10.7
	0.031–0.040	11.4	3.2	3.0
	>0.041	9.6	0.6	0.0
CBD_{Ladder} (kg m^{-3})				
	0.000–0.010	1.6	0.0	0.0
	0.011–0.020	22.4	31.4	19.7
	0.021–0.030	40.3	58.5	78.4
	0.031–0.040	20.2	9.4	1.9
	>0.041	15.5	0.7	0.0

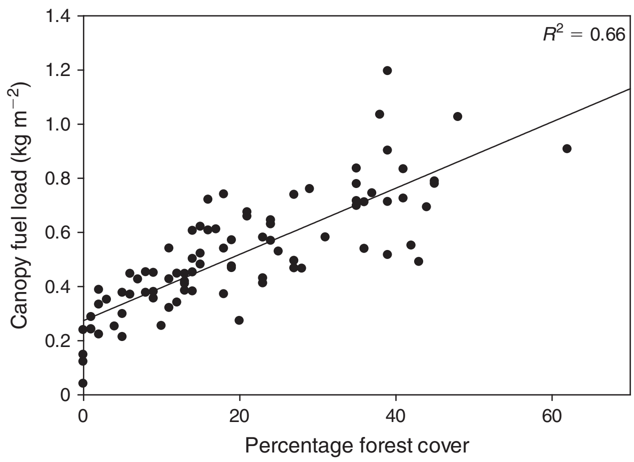

Fig. 5. Scatter-plot of percentage forest cover vs ALS-estimated CFL for B_{30}.

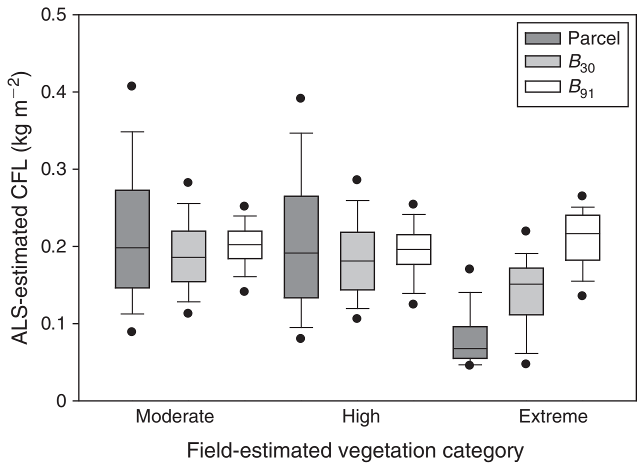

Fig. 6. Boxplot of field-estimated fuel class to ALS-estimated CFL for Parcels, B_{30} and B_{91} ($n = 1901$, 310 and 121 for 'moderate', 'high' and 'extreme' respectively.)

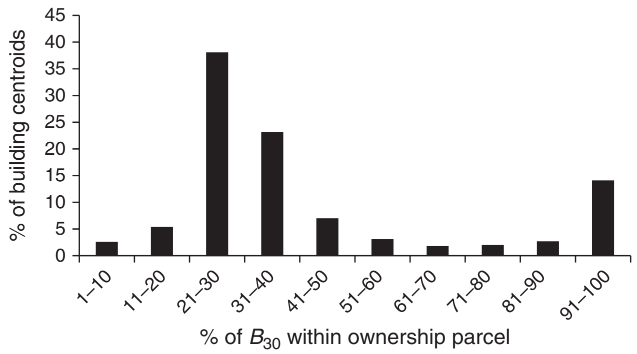

Fig. 7. Percentage of B_{30} within the related ownership parcel.

Based on our 'relative' risk assessment, over 25% of the structure centroids had a rating of 'high', which is the highest risk rating (Table 5). The spatial presentation of these results clearly demonstrates the impact that targeted management activities could have on the structural groupings that have received the higher risk ratings (Fig. 8*a*).

Discussion

The motivation for the present work was to develop an objective methodology for integrating ALS and spectral reflectance datasets into structure-level wildland fire risk assessments for WUI areas. Broadly, our results suggest that our remote-sensing approach can augment, and improve on, field-based approaches by providing more quantitative and accurate estimates of the variables relevant to the assessment of risk for individual structures to wildland fire. We have found that integration area has a large influence on the expression of fuel loading and cover characteristics. For our study area, there was a trend towards homogenisation of fuel loadings and forest cover characteristics as the size of the assessment area increased. Our results also indicate that ALS datasets are useful for quantifying fuel loading within the HIZ and allow the ranking of risk in a way that is complementary to many field-based fuel-assessment

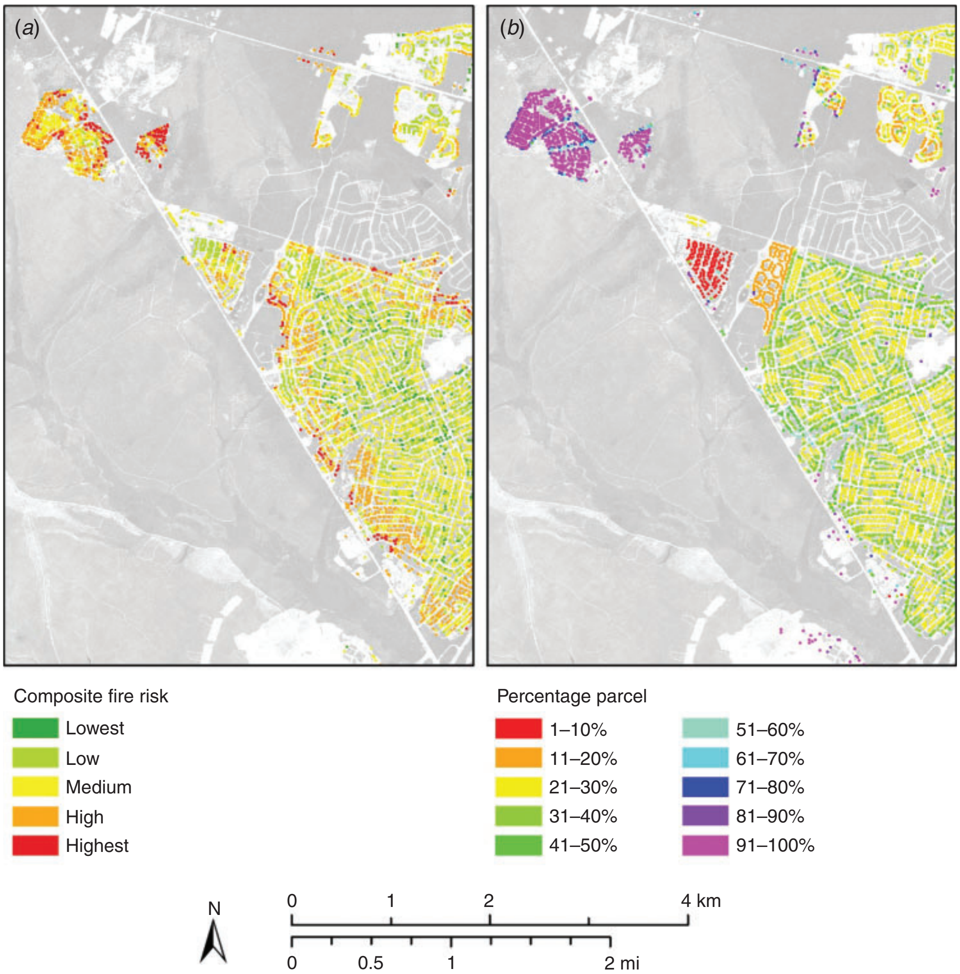

Fig. 8. Maps of composite fire risk (*a*); and percentage of B_{30} within the ownership parcel (*b*).

Table 5. Percentage of structure centroids by relative risk category

Risk class	% of centroids
Lowest	4.2
Low	25.4
Medium	42.4
High	22.9
Highest	5.0

methodologies. An additional important finding was that owners of a majority of the parcels (individual homeowners) in our study area were unable to control the vegetation within their respective HIZ without the cooperation of adjacent property owners. The findings of this study are important because the methodology provides the framework for a standardised supplement, or alternative, to ground-based structural fire assessments that can be implemented over broad spatial scales.

The area of consideration for fire risk surrounding individual structures has been well defined in the literature. For example, a recent study by Gibbons *et al.* (2012) used the 2009 wildfires in southern Australia as a test case to evaluate which variables are factors in structure loss. Using an empirical methodology, they developed relationships between several explanatory variables and found the most significant variable predicting structure ignition was vegetative cover within 40 m of structures. These results reinforce the concept of the HIZ presented by Cohen (2000), developed as a result of modelling and experimentation at the International Crown Fire Modelling Experiment (Stocks *et al.* 2004). As such, we originally chose to analyse the data using the B_{30} and B_{91} buffers around each structure. In the high-density WUI areas within our study area, integrating over these areas often led to the inclusion of impervious surfaces (e.g. Figs 2 and 3), which led to lower estimates of fuel loading and pine cover around these structures. The parcel-level analysis resulted in distributions with higher mean estimates and larger standard deviations for each of the fuel loading components compared with the B_{30} and B_{91} estimates. It is conceivable that because the average parcel size in our study area was less than the mean area of B_{30} or B_{91}, this finding may not be applicable in landscapes with larger parcel sizes and grouping by parcel would lead to greater homogeneity of fuel estimates.

This finding suggests that the scale of analyses is an important consideration when systematically ranking risk in communities, because a fixed analysis window may be confounded in areas where there are varying road densities and parcel sizes.

The vertical fuel structure that can be derived from ALS datasets make it a well-suited tool for estimating fuel classes (e.g. Koetz *et al.* 2008; Mutlu *et al.* 2008; Jakubowksi *et al.* 2013) and loading in forested areas (e.g.Andersen *et al.* 2005; Hermosilla *et al.* 2013). However, fewer studies incorporated these datasets into fuel estimates in the HIZ. In one example, Platt (2014) used a fusion approach with ALS, spectral reflectance and building footprint data for the classification of fuels and other parameters within the HIZ. He also included a variable that characterised ladder fuels as a percentage of first returns between 1 and 3 m. To our knowledge, our study represents the first effort that has used ALS data to estimate canopy fuel parameters (e.g. CBD_{max}, CDB_{Ladder} and CLF) within the HIZ. There are few studies, therefore, to compare our estimated loadings with. However, estimates are available for wildland fuels on this landscape. Skowronski *et al.* (2011) reported mean CFLs in several stands of contiguous forest of similar species composition approximately 5 km north of our study area that were an order of magnitude greater than those presented here. Thus, it merits further study to determine whether these ranges of fuel loadings area are a result of models that do not accurately represent the loadings found in the WUI area, or if the low fuel loadings here are a reflection of the heterogeneity of impervious surfaces, houses and lawns.

Although the present study has focussed on the estimation of fuels within the HIZ as specified by the NFPA (NFPA 2012), the methods presented here can be easily adapted to other systems that use an area or parcel-based sampling approach to assess risk around individual structures. For example, the Canadian 'Fire-Smart' program presents a 'Wildfire Hazard Assessment System' that specifies several radial distances from homes (<10, 10–30 and 30–100 m) and several variables similar to those examined here (forest composition, ladder fuels, surface vegetation; www.firesmartcanada.ca/). In addition, in Australia, the New South Wales Rural Fire Service has recently implemented a 'Bush Fire Household Assessment Tool' that uses several variables similar to those presented here and also includes a calculator that estimates the impacts that adjacent parcels may have on a structure's HIZ similarly to the data presented here (O'Halloran 2014). In the context of these types of hazard assessment systems, the method presented here allows the targeted assessment of individual structures for the development of a broad assessment similar to that of the flood assessment program administered by the US Federal Emergency Management Agency (FEMA). The FEMA flood-hazard mapping program (FEMA 2013) maps and assesses flood hazard for individual structures through the United States with an approach that makes use of cadastral data coupled with an integrated flood-modelling approach. The data products that result from these assessments provide a decision-support system that can inform many scales of policy and decision-making while also providing a consistent reference for the insurance (National Flood Insurance Program; FEMA 2013) and home-construction industries, and for individuals exploring property transactions.

There are several limitations associated with the methodology presented here. First, the expense of ALS data, although decreasing over time, currently limits its utility in this type of application. However, prioritising problem areas using coarse-grained information like that from the Rapid Assessment of Values at Risk program (RAVAR; www.fs.fed.us/rm/wfdss_ravar/), could be used to guide decisions about where it is necessary characterise fuels at a finer scale. Even in the cases where data were available, changes to the landscape would require periodic updates to the dataset. Specific computational tools and technical expertise are required to perform the required processing operations, to delineate building footprints and to synthesise data products. Models would also need to be developed to link species-specific fuel characteristics to ALS attributes (e.g. Skowronski *et al.* 2011; Clark *et al.* 2013), although it is likely that a non-dimensional 'relative loading' would be appropriate for the ranking of risk in some situations. Although we present a generalised 'risk' model here to serve as a simple integrator of the data products that we have developed, a full assessment of structure risk would also include other variables including response time, probability of spread between homes, building materials and fire-brand spotting (Haas *et al.* 2013). These factors could have been added as components to the model, but we chose the factors that are both relevant and essential to understand the fuel environment around individual structures.

Conclusions

The goal of this study was to develop and apply emerging remote-sensing products and analysis techniques to improve our ability to map hazard and characterise risk in the WUI. More specifically, our objective was to develop and evaluate a methodology that allows the assessment of wildland fuels on an individual structure basis. The strength of this methodology is that it provides spatial estimates of fire risk for fire-management operations and broader policy-level analysis while also providing actionable information for individual building owners. The remotely sensed methodology appears to display greater sensitivity in characterising fuel loading as compared with the field-based fuel survey. Additionally, the results of our study indicate that the size of the areal sampling unit can have an effect on the expression of the variables around individual structures as housing density and impervious surfaces impact these analyses. In our study area, we also found that there are a large proportion of homes that are unable to manage hazardous fuels within the HIZ without the cooperation of adjacent property owners. We suggest that this or a similar methodology can be easily scaled to provide regional assessments. The knowledge gained in this study can help guide risk-mitigation practices and zoning policy and serve as a pilot to future large-scale studies.

Acknowledgements

We thank Gregory McLaughlin and Trevor Raynor of the NJFFS for access to survey data. This work was funded by USDA Forest Service Northern Research Station and Rutgers, The State University of New Jersey Agricultural Experiment Station through agreement no. 09-JV-11242306–075, USDI Joint Fire Sciences Program (project no. 10–1-02–14), and an interagency agreement between the New Jersey Air National Guard and the USDA Forest Service Northern Research Station (agreement no. 112423).

References

Alonso-Benito A, Arroyo LA, Arbelo M, Hernández-Leal P, González-Calvo A (2013) Pixel and object-based classification approaches for mapping forest fuel types in Tenerife Island from ASTER data. *International Journal of Wildland Fire* **22**, 306–317. doi:10.1071/WF11068

Andersen HE, McGaughey RJ, Reutebuch SE (2005) Estimating forest canopy fuel parameters using LiDAR data. *Remote Sensing of Environment* **94**, 441–449. doi:10.1016/J.RSE.2004.10.013

Anderson HE (1982) Aids to determining fuel models for estimating fire behavior. USDA Forest Service, Intermountain Forest and Range Experiment Station, General Technical Report INT-GTR-122. (Ogden, UT).

Arroyo L, Pascual C, Manzanera J (2008) Fire models and methods to map fuel types: the role of remote sensing. *Forest Ecology and Management* **256**, 1239–1252. doi:10.1016/J.FORECO.2008.06.048

Berry AH, Hesseln H (2004) The effect of the wildland–urban interface on prescribed burning costs in the Pacific North-western United States. *Journal of Forestry* **102**(6), 33–37.

Breiman L (2001) Random forests. *Machine Learning* **45**(1), 5–32. doi:10.1023/A:1010933404324

Chen Q (2007) Airborne lidar data processing and information extraction. *Photogrammetric Engineering and Remote Sensing* **73**, 109–112.

Clark KL, Skowronski NS, Gallagher MG, Carlo N, Farrell M, Maghirang M (2013) Assessment of canopy fuel loading across a heterogeneous landscape using LiDAR, JFSP final report 10–1-02–14. Available at https://www.firescience.gov/projects/10-1-02-14/project/10-1-02-14_final_report.pdf [Verified 22 July 2015]

Cohen JD (2000) Preventing disaster: home ignitability in the wildland–urban interface. *Journal of Forestry* **98**, 15–21.

Cohen JD (2008) The wildland–urban interface fire problem *Forest History Today* **Fall**, 20–26http://www.fs.fed.us/rm/pubs_other/rmrs_2008_cohen_j002.pdf.

Erdody TL, Moskal LM (2010) Fusion of LiDAR and imagery for estimating forest canopy fuels. *Remote Sensing of Environment* **114**(4), 725–737. doi:10.1016/J.RSE.2009.11.002

Federal Emergency Management Agency (FEMA) (2013) Guidelines and specifications for flood hazard mapping partners. FEMA's Flood Hazard Mapping Program, Washington, DC. National Flood Insurance Program: Flood Insurance Manual, Revised January, 2013. Federal Emergency Management Agency (FEMA) (Washington, DC) Available at http://www.fema.gov/media-library/assets/documents/29840?id=6713 [Verified 22 July 2015]

Forman RT, Boerner RE (1981) Fire frequency and the Pine Barrens of New Jersey. *Bulletin of the Torrey Botanical Club* **108**(1), 34–50. doi:10.2307/2484334

Gibbons P, van Bommel L, Gill AM, Cary GJ, Driscoll DA, Bradstock RA, Knight E, Moritz MA, Stephens SL, Lindenmayer DB (2012) Land management practices associated with house loss in wildfires. *PLoS One* **7**(1), e29212. doi:10.1371/JOURNAL.PONE.0029212

Gorte RW (2011) Federal funding for wildfire control and management. Available at http://digital.library.unt.edu/ark:/67531/metadc96772/m1/1/high_res_d/RL33990_2011Jul05.pdf [Verified 22 July 2015]

Haas JR, Calkin DE, Thompson MP (2013) A national approach for integrating wildfire simulation modeling into wildland–urban interface risk assessments within the United States. *Landscape and Urban Planning* **119**, 44–53. doi:10.1016/J.LANDURBPLAN.2013.06.011

Hermosilla T, Ruiz LA, Kazakova AN, Coops NC, Moskal LM (2013) Estimation of forest structure and canopy fuel parameters from small-footprint full-waveform LiDAR data. *International Journal of Wildland Fire* **23**, 224–233. doi:10.1071/WF13086

Jakubowksi MK, Guo Q, Collins B, Stephens S, Kelly M (2013) Predicting surface fuel models and fuel metrics using Lidar and CIR imagery in a dense, mountainous forest. *Photogrammetric Engineering and Remote Sensing* **79**, 37–49. doi:10.14358/PERS.79.1.37

Koetz B, Morsdorf F, Van der Linden S, Curt T, Allgöwer B (2008) Multisource land-cover classification for forest fire management based on imaging spectrometry and LiDAR data. *Forest Ecology and Management* **256**, 263–271. doi:10.1016/J.FORECO.2008.04.025

La Puma IP, Lathrop RG, Keuler NS (2013) A large-scale fire suppression edge-effect on forest composition in the New Jersey Pinelands. *Landscape Ecology* **28**, 1815–1827. doi:10.1007/S10980-013-9924-7

Liang J, Calkin DE, Gebert KM, Venn TJ, Silverstein RP (2008) Factors influencing large wildland fire suppression expenditures. *International Journal of Wildland Fire* **17**, 650–659. doi:10.1071/WF07010

MacArthur RH, Horn HS (1969) Foliage profiles by vertical measurement. *Ecology* **50**, 802–804. doi:10.2307/1933693

McCaffrey S, Toman E, Stidham M, Shindler B (2012) Social science research related to wildfire management: an overview of recent findings and future research needs. *International Journal of Wildland Fire* **22**, 15–24. doi:10.1071/WF11115

McCormick J, Jones L (1973) The Pine Barrens: vegetation geography. New Jersey State Museum, Research Report Number 3. (New Jersey State Museum: Trenton, NJ)

Mell WE, Manzello SL, Maranghides A, Butry D, Rehm RG (2010) The wildland–urban interface problem – current approaches and research needs. *International Journal of Wildland Fire* **19**, 238–251. doi:10.1071/WF07131

Mutlu M, Popescu SC, Stripling C, Spencer T (2008) Mapping surface fuel models using Lidar and multispectral data fusion for fire behavior. *Remote Sensing of Environment* **112**, 274–285. doi:10.1016/J.RSE.2007.05.005

NFPA (2010) Deadliest/large-loss fires, 25 largest fire losses in US history. (National Fire Protection Association: Quincy, MA) Available at http://www.nfpa.org/itemDetail.asp?categoryID=954&itemID=23352&URL=Research/Fire%20statistics/Deadliest/large-loss%20fires

NFPA (2012) NFPA 1144: standard for reducing structure ignition hazards from wildland fire. 2013 edn (National Fire Protection Association: Quincy, MA) Available at http://www.nfpa.org/AboutTheCodes/AboutTheCodes.asp?DocNum=1144

O'Halloran M (2014) NSW RFS Bush Fire Household Assessment Tool. In 'Research forum 2014: proceedings of the research forum at the Bushfire and Natural Hazards CRC & AFAC conference', 2 September 2014, Wellington, New Zealand. (Ed. M. Rumsewicz) pp. 190–197 (Bushfire and Natural Hazards CRC: Melbourne, Vic.)

Pinelands Commission (1980) 'New Jersey Pinelands comprehensive management plan.' (Pinelands Commission: New Lisbon, NJ)

Platt RV (2014) Wildfire hazard in the home ignition zone: an object-oriented analysis integrating LiDAR and VHR satellite imagery. *Applied Geography* **51**, 108–117. doi:10.1016/J.APGEOG.2014.03.011

Scott JH, Burgan RE (2005) Standard fire behavior fuel models: a comprehensive set for use with Rothermel's surface fire spread model. USDA Forest Service, Rocky Mountain Research Station, General Technical Report RMRS-GTR-153. (Fort Collins, CO)

Skowronski NS, Clark KL, Nelson R, Hom J (2007) Remotely sensed measurements of forest structure and fuel load in the Pinelands of New Jersey. *Remote Sensing of Environment* **108**(2), 123–129. doi:10.1016/J.RSE.2006.09.032

Skowronski NS, Clark KL, Duveneck M, Hom J (2011) Three-dimensional canopy fuel loading predicted using upward and downward sensing LiDAR systems. *Remote Sensing of Environment* **115**(2), 703–714. doi:10.1016/J.RSE.2010.10.012

Stocks BJ, Alexander ME, Lanoville RA (2004) Overview of the international crown fire modelling experiment (ICFME). *Canadian Journal of Forest Research* **34**, 1543–1547. doi:10.1139/X04-905

Tedrow JCF (1986) 'Soils of New Jersey. New Jersey Agricultural Experiment Station, Publication A-15134–1-82.' (Krieger Publishing Co.: Malabar, FL)